Ultra-low power, Zeno effect based optical modulation in a degenerate V-system with a tapered nano fiber in atomic vapor

K. Salit,[1] M. Salit,[2] Subramanian Krishnamurthy,[1] Y. Wang,[1] P. Kumar,[1,2] and M. S. Shahriar[1,2,*]

[1]*Department of EECS, Northwestern University, Evanston, IL 60208, USA*
[2]*Department of Physics and Astronomy, Northwestern University, Evanston, IL 60208, USA*
**shahriar@northwestern.edu*

Abstract: We demonstrate an ultra-low light level optical modulator using a tapered nano fiber embedded in a hot rubidium vapor. The control and signal beams are co-propagating but orthogonally polarized, leading to a degenerate V-system involving coherent superpositions of Zeeman sublevels. The modulation is due primarily to the quantum Zeno effect for the signal beam induced by the control beam. For a control power of 40 nW and a signal power of 100 pW, we observe near 100% modulation. The ultra-low power level needed for the modulation is due to a combination of the Zeno effect and the extreme field localization in the evanescent field around the taper.

OCIS codes: (190.4370) Nonlinear optics, fibers; (250.4110) Modulators.

References and links

1. S. E. Harris and Y. Yamamoto, "Photon switching by quantum interference," Phys. Rev. Lett. **81**(17), 3611–3614 (1998).
2. R. G. Beausoleil, W. J. Munro, D. A. Rodrigues, and T. P. Spiller, "Applications of electromagnetically induced transparency to quantum information processing," J. Mod. Opt. **51**(16-18), 2441–2448 (2004).
3. A. M. C. Dawes, L. Illing, S. M. Clark, and D. J. Gauthier, "All-optical switching in rubidium vapor," Science **308**, 672–674 (2005).
4. Q. Xu and M. Lipson, "All-optical logic based on silicon micro-ring resonators," Opt. Express **15**(3), 924–929 (2007).
5. M. Bajcsy, S. Hofferberth, V. Balic, T. Peyronel, M. Hafezi, A. S. Zibrov, V. Vuletic, and M. D. Lukin, "Efficient all-optical switching using slow light within a hollow fiber," Phys. Rev. Lett. **102**(20), 203902 (2009).
6. V. Venkataraman, P. Londero, A. R. Bhagwat, A. D. Slepkov, and A. L. Gaeta, "All-optical modulation of four-wave mixing in an Rb-filled photonic bandgap fiber," Opt. Lett. **35**(13), 2287–2289 (2010).
7. S. M. Spillane, G. S. Pati, K. Salit, M. Hall, P. Kumar, R. G. Beausoleil, and M. S. Shahriar, "Observation of nonlinear optical interactions of ultralow levels of light in a tapered optical nanofiber embedded in a hot rubidium vapor," Phys. Rev. Lett. **100**(23), 233602 (2008).
8. G. Brambilla, V. Finazzi, and D. J. Richardson, "Ultra-low-loss optical fiber nanotapers," Opt. Express **12**(10), 2258–2263 (2004).
9. S. M. Hendrickson, M. M. Lai, T. B. Pittman, and J. D. Franson, "Observation of two-photon absorption at low power levels using tapered optical fibers in rubidium vapor," Phys. Rev. Lett. **105**(17), 173602 (2010).
10. T. A. Birks, W. J. Wadsworth, and P. St. J. Russell, "Supercontinuum generation in tapered fibers," Opt. Lett. **25**(19), 1415–1417 (2000).
11. S. M. Spillane, T. J. Kippenberg, O. J. Painter, and K. J. Vahala, "Ideality in a fiber-taper-coupled microresonator system for application to cavity quantum electrodynamics," Phys. Rev. Lett. **91**(4), 043902 (2003).
12. D. J. Alton, N. P. Stern, T. Aoki, H. Lee, E. Ostby, K. J. Vahala, and H. J. Kimble, "Strong interactions of single atoms and photons near a dielectric boundary," Nat. Phys. **7**(2), 159–165 (2011).
13. T. Allsop, F. Floreani, K. P. Jedrzejewski, P. V. S. Marques, R. Romero, D. J. Webb, and I. Bennion, "Spectral characteristics of tapered LPG device as a sensing element for refractive index and temperature," J. Lightwave Technol. **24**(2), 870–878 (2006).
14. J. Villatoro and D. Monzón-Hernández, "Fast detection of hydrogen with nano fiber tapers coated with ultra thin palladium layers," Opt. Express **13**(13), 5087–5092 (2005).

#151983 - $15.00 USD Received 15 Aug 2011; revised 27 Sep 2011; accepted 3 Oct 2011; published 27 Oct 2011

15. K. P. Nayak, F. L. Le Kien, M. Morinaga, and K. Hakuta, "Antibunching and bunching of photons in resonance fluorescence from a few atoms into guided modes of an optical nanofiber," Phys. Rev. A **79**(2), 021801(R) (2009).
16. V. G. Minogin and S. N. Chormaic, "Manifestation of the van der Waals Surface Interaction in the Spontaneous Emission of Atoms into an Optical Nanofiber," Laser Phys. **20**(1), 32–37 (2010).
17. E. Vetsch, D. Reitz, G. Sagué, R. Schmidt, S. T. Dawkins, and A. Rauschenbeutel, "Optical interface created by laser-cooled atoms trapped in the evanescent field surrounding an optical nanofiber," Phys. Rev. Lett. **104**(20), 203603 (2010).
18. S. Weis, R. Rivière, S. Deléglise, E. Gavartin, O. Arcizet, A. Schliesser, and T. J. Kippenberg, "Optomechanically Induced Transparency," Science **330**(6010), 1520–1523 (2010).
19. J. M. Ward, Y. Wu, V. G. Minogin, and S. N. Chormaic, "Trapping of a microsphere pendulum resonator in an optical potential," Phys. Rev. A **79**(5), 053839 (2009).
20. S. Ghosh, A. R. Bhagwat, C. K. Renshaw, S. Goh, A. L. Gaeta, and B. J. Kirby, "Low-Light-Level Optical Interactions with Rubidium Vapor in a Photonic Band-Gap Fiber," Phys. Rev. Lett. **97**(2), 023603 (2006).
21. W. Yang, D. B. Conkey, B. Wu, D. Yin, A. R. Hawkins, and H. Schmidt, "Atomic spectroscopy on a chip," Nat. Photonics **1**(6), 331–335 (2007).
22. B. Misra and E. C. G. Sudarshan, "The Zeno's paradox in quantum theory," J. Math. Phys. **18**(4), 756–763 (1977).
23. W. M. Itano, D. J. Heinzen, J. J. Bollinger, and D. J. Wineland, "Quantum Zeno Effect," Phys. Rev. A **41**(5), 2295–2300 (1990).
24. Y. Huang, J. B. Altepeter, and P. Kumar, "Interaction-free all-optical switching via the quantum Zeno effect," Phys. Rev. A **82**(6), 063826 (2010).
25. C. Cohen-Tannoudji, S. Reynaud; "Dressed-atom description of resonance fluorescence and absorption spectra of a multi-level atom in an intense laser beam," J. Phys. B **10**(3), 345–363 (1977) (old 16).
26. E. R. I. Abraham and E. A. Cornell, "Teflon feedthrough for coupling optical fibers into ultrahigh vacuum systems," Appl. Opt. **37**(10), 1762–1763 (1998).
27. B. V. Zhdanov and R. J. Knize, "Progress in alkali lasers development," Proc. SPIE **6874**, 68740F, 68740F-12 (2008) (and references therein).
28. S. M. Hendrickson, T. B. Pittman, and J. D. Franson, "Nonlinear transmission through a tapered fiber in rubidium vapor," J. Opt. Soc. Am. B **26**(2), 267 (2009).

1. Introduction

All-optical modulation and switching are important for optical communication and quantum information processing [1–6]. Conventional techniques of non-linear optics typically require relatively high power, and are not well suited for these applications. In recent years, several innovative techniques for modulation and switching have been demonstrated at very low power. These include, for example, techniques based on instability-induced processes in atomic vapor [3], silicon micro ring resonators [4], and hollow-core fibers [5,6]. Here, we report an all optical modulator which can operate at a power level much lower than any other technique demonstrated so far. Specifically, we use a tapered nano fiber (TNF) [7–9] embedded in Rb vapor to produce ultra-low power modulation via the quantum Zeno effect. The fact that many such modulators may be realizable on a chip-scale vapor cell makes this an attractive technology for optical communication. The TNF-based modulator could also be integrated with other applications of TNF such as super-continuum generation [10], coupling light into micro-sphere resonators [11,12], near-field sensing [13,14], investigation of interaction of evanescent field with cold atoms [15–17], and exploration of opto-mechanical effects [18,19].

Two important factors have come together to produce such an efficient modulator. First, the TNF provides a unique combination of extremely small effective mode area of ~0.2 μm^2 [7] and interaction length of ~5 mm. In contrast, the hollow-core fiber [20] and the Arrow waveguide [21] have mode areas of about 100 μm^2 and 6.7 μm^2, respectively, but allow for large interaction lengths. However, the TNF is long enough to produce complete absorption in a vapor at a temperature of about 100° C, thus making high-contrast modulation feasible. Second, we make use of the quantum Zeno effect, which controls the absorption of a signal beam via pump-induced modification of absorption, rather than refraction, thus making it inherently very efficient.

#151983 - $15.00 USD Received 15 Aug 2011; revised 27 Sep 2011; accepted 3 Oct 2011; published 27 Oct 2011

2. Quantum Zeno effect

In the most general sense, the quantum Zeno effect (QZE) [22–24] refers to the evolution (or suppressed evolution) of a quantum state through the quantum measurement process. The term itself was coined to describe the suppression of an atomic transition. Figure 1 (a) shows the energy level diagram of a three level system to illustrate this process. Here, states |1> and |2> are assumed long-lived, while state |3> decays rapidly, at a rate Γ, into state |1> only. The 1-2 coupling is assumed to be weak. The QZE in this configuration can be explained as follows. In the absence of any coupling to state |3>, state |1> will undergo Rabi oscillation, thus getting excited to state |2> at a rate determined by the 1-2 coupling strength. When coupled to state |3>, the spontaneous emission emulates a measurement process (without requiring an actual measurement), which resets the quantum state of the system to state |1>. As such, evolution of state |1> into state |2> is inhibited, locking the electron in state |1> indefinitely. Viewed as a switch, the collapsed state |1> is switch output one. Complete evolution into state |*2*> is switch output two.

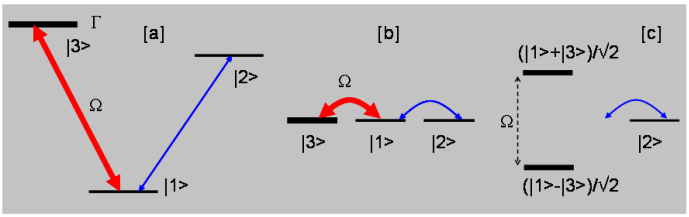

Fig. 1. The quantum Zeno effect for atomic transitions. The state |1> is weakly coupled to|2>, but this evolution is continuously suppressed by the presence of a pump laser coupling |1> to |3>

The fact that no actual measurement is necessary implies that the QZE is fully contained within the conventional description of this process, based on the Liouvillian evolution of the density matrix. As such, it is possible to provide a simpler interpretation of the QZE in terms of level-splitting. To see this, note first that when the energies of the photons are taken into account, this process can be represented by the so-called dressed states, which are degenerate for resonant excitations, as illustrated in Fig. 1(b) [25]. If the interaction between states |1> and |3> is diagonalized, states |1> and |3> are replaced by two quasi-eigenstates, representing in-phase and out-of phase superpositions thereof. This is illustrated in Fig. 1(c). Since each one of these quasi-eigenstates is now non-degenerate with state |2>, with a splitting equaling the 1-3 coupling rate (Ω) much larger than the 1-2 coupling rate, the excitation to |2> is suppressed. Residual excitation to state |2> can still occur due to the finite overlap between the split levels (due to the linewidths), as well as due to the transit time broadening of the 1-2 coupling. This picture remains valid even if the 1-3 coupling is pulsed; in that case, the splitting is convolved with the spectrum of the pulse pattern. If this convolution produces a component that is degenerate with state |2>, then the suppression is reduced. This is consistent with the fact that the QZE suppression is most efficient when the 1-3 coupling is continuous.

3. TNF system setup

In the experiment reported here, we combine the QZE with a TNF to demonstrate an ultra low-power modulator. Briefly, the TNF is made by oxy-hydrogen flame-heating and pulling of a standard single-mode fiber into a narrow thread over a length of a few millimeters. During the tapering process, in situ monitoring of fiber transmission shows negligible loss due to the taper. SEM imaging was used to measure the diameter of the tapered section to be around ~400 nm. The effective mode area of the fiber was inferred to be about 0.2 μm^2, based on the model summarized in Ref. [7]. In order to load the fiber into the vacuum chamber, the tapered section of the fiber was laid on a custom-made copper chuck and held fixed using a

#151983 - $15.00 USD Received 15 Aug 2011; revised 27 Sep 2011; accepted 3 Oct 2011; published 27 Oct 2011

small dab of UV-curable epoxy at both ends away from the taper. The chuck was then mounted on a straight copper tube with a Swagelock® fitting on one end. The fiber was passed through the fitting with the help of a hole in a Teflon® ferrule [26], which was used to vacuum-seal the chamber by compression. The other end of the fiber was also taken out of the chamber using a similar fitting and ferrule combination at the bottom of the chamber. A vacuum sealant was sprayed at the fiber-ferrule joint in order to achieve a pressure of about 5 mTorr. The copper tube was heated from outside to reach a temperature of 100°C. The vacuum chamber was also heated to the same temperature. Between experimental runs, the oven was kept isolated from the TNF chamber with an all metal valve. This apparatus is shown schematically in Fig. 2.

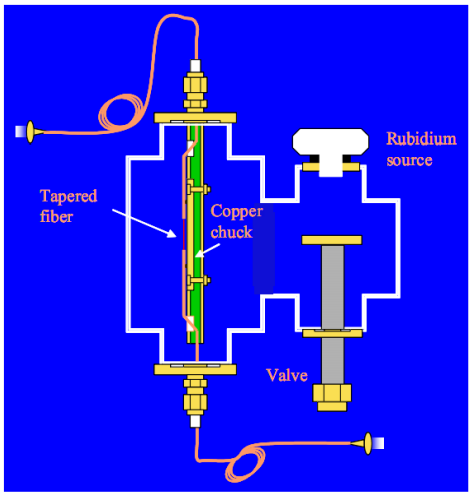

Fig. 2. Schematic of the tapered Nano fiber set-up

4. Experimental setup

The experimental setup is summarized in Fig. 3. The output of a Ti:Sapphire laser was split by a 50/50 non-polarizing beam splitter. The beam reflected by the splitter was shifted up by 80 MHz with an acousto-optic modulator (AOM), to produce the S-polarized probe beam. The beam passing through the splitter was up-shifted by a second AOM, also at 80 MHz, to produce the pump beam, which was P-polarized by passing through a half-wave plate. Attenuators were then used to reduce the power in both beams independently. The pump and probe were combined on a polarizing beam-splitter (PBS), and coupled into the TNF. The output was passed through another PBS, separating out the pump and the probe. The probe was then detected with an avalanche photo-diode (APD). Using another non-polarizing beam splitter, 10% of the probe beam (before attenuation) was diverted to a vapor cell for saturated absorption spectroscopy. For the pulsed modulation reported in section 5.2, signal from this cell was used to lock the laser to a hyperfine transition.

5. Results

5.1 Probe absorption reduction due to presence of pump

Figure 4 shows one set of data taken using this setup. The probe (pump) power was 100 pW (40 nW). First, the red trace shows the probe transmission when the pump beam is turned off. As the probe frequency was scanned across the D1 manifold, three dips were observed. The biggest dip corresponds to the transition from the $5S_{1/2}$, $F = 3$ ground-state in ^{85}Rb to the $5P_{3/2}$ hyperfine levels, which are not resolved because of Doppler broadening. The small dip on its

#151983 - $15.00 USD Received 15 Aug 2011; revised 27 Sep 2011; accepted 3 Oct 2011; published 27 Oct 2011

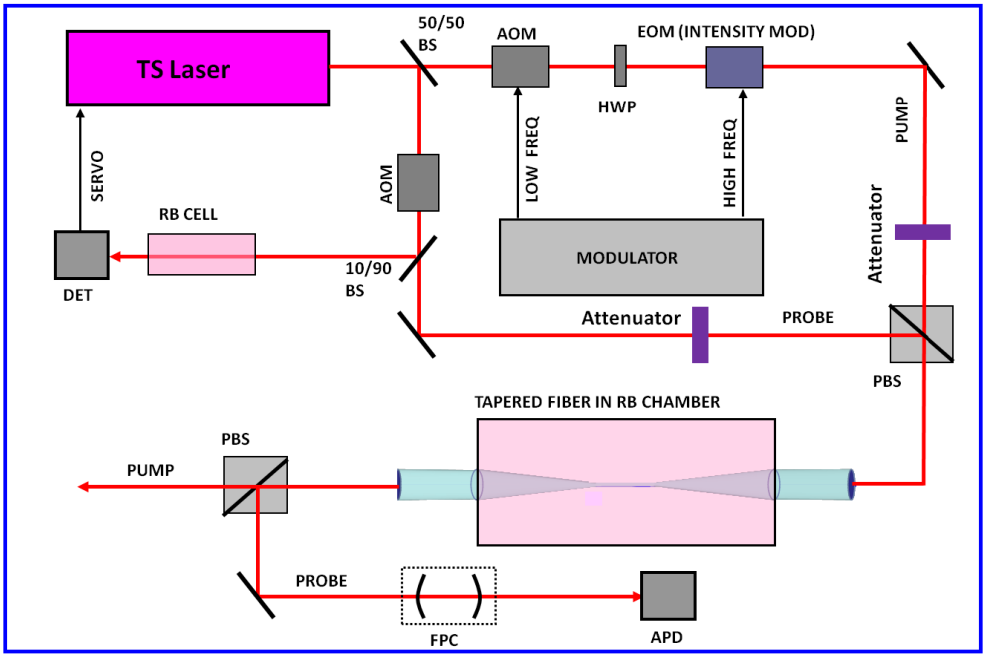

Fig. 3. Experimental setup for demonstrating optical modulation. Both AOMs are operated at the same frequency (80 MHz). The pump and the probe are each linearly polarized, orthogonal to each other.

left corresponds to a transition in ^{87}Rb, from $5S_{1/2}$, $F = 2$ ground-state to the $5P_{3/2}$ hyperfine levels. The dip on its right corresponds to the transition from the $5S_{1/2}$, $F = 2$ ground-state in ^{85}Rb to the $5P_{3/2}$ hyperfine levels. The scan range was not long enough to see the other transition in ^{87}Rb: from $5S_{1/2}$, $F = 1$ ground-state to the $5P_{3/2}$ hyperfine levels.

Next, the blue trace shows the probe absorption when the pump is turned on. There is a strong increase in the probe transmission at the center of the $F = 3$ transition (the middle one

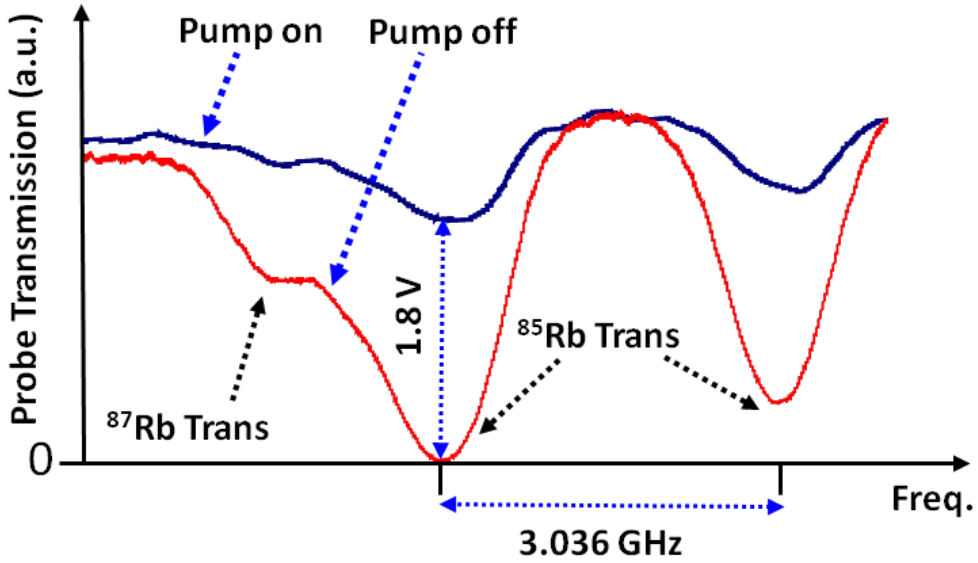

Fig. 4. Absorption spectrum of the probe in the absence (red) and presence (blue) of the pump.

#151983 - $15.00 USD Received 15 Aug 2011; revised 27 Sep 2011; accepted 3 Oct 2011; published 27 Oct 2011

in Fig. 4). The physical mechanism behind the strong modulation of the probe transmission caused by the pump can be explained as follows. Consider first the Zeeman sublevel of the $m_F = 0$ in the $F = 3$ ground-state, and how it is coupled to the $F' = 2$ excited state. The probe, which is a superposition of left and right circularly polarized light, with a relative phase ψ, would couple this state to $m_F = -1$ and $m_F = 1$ sublevels in the $F' = 2$ state. The pump is also a superposition of left and right circularly polarized light, with a relative phase ϕ, and would excite the same pair of transitions.

However, the phases ψ and ϕ differ by π. As such, the net interaction can be represented as a V-system, with one leg excited by the probe and the other by the pump. This is illustrated in Fig. 5. Here, the in-phase superposition state (|p>) is coupled to the ground state |a> by the P-polarized pump beam only, and the out-of-phase superposition state (|n>) is coupled to the ground state |a> by the S-polarized probe beam only. Thus, the net interaction is equivalent to the V-system shown in Fig. 1, in the same configuration as what corresponds to the QZE. Specifically, in the absence of the pump, the probe excites state |a> to state |n>, corresponding to strong absorption. However, when the pump is present, the effective continuous measurement process keeps the atoms locked in state |a>, thus reducing strongly the absorption of the probe beam.

It should be noted that when the pump is turned on, the residual probe absorption develops some asymmetry, and the centroid of each dip appears to be slightly shifted. Further investigation is required to elucidate the origin of these effects, and will be carried out in the future. However, for the purpose of modulation, these effects may not be very important.

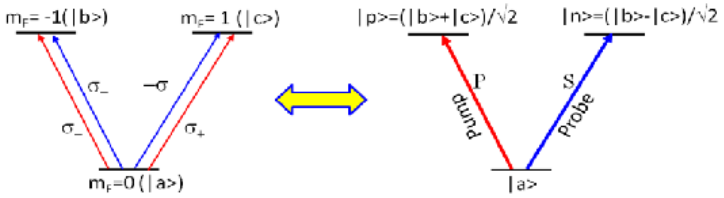

Fig. 5. Schematic illustration of the process that produces the QZE when the atoms are excited by cross-linearly polarized pump and probe beams.

A more quantitative description of the process makes use of the concept of level splitting, as also described in the introduction. Specifically, when the pump is turned on, the ground state gets split into two dressed states, each out of resonance for the probe if the pump intensity is greater than the saturation intensity of the isolated atom (i.e., $\Omega > \Gamma$, where Ω is the pump Rabi frequency, and Γ is the natural linewidth). When the Doppler broadening is taken into account, the condition for probe transparency is that $\Omega > \sqrt{(\Gamma * \Gamma_D)}$, where Γ_D is the half-width of the Doppler broadening. This condition is satisfied by the pump power (~40 nW) used. The same model applies to transitions to the $F' = 3$ and $F' = 4$ excited states as well. Of course, for some values of m_F, only left (right) circular transition is allowed; in that case, the system behaves as a pure two level transition, excited by identically polarized parts of the pump and the probe. The reduction in probe transmission for these sublevels is due to the conventional self-induced transparency.

5.2 Pulsed modulation

Figure 6 shows results of pulsed modulation, with the laser locked at the center of the $F = 3$ transition. The probe is kept constant at 100 pW, while the pump intensity is modulated by using the pump AOM. The top left panel shows the probe transmission when this modulation is at 10 Hz. The other three panels show the same for increasing modulation frequencies. At 10 KHz, the probe transmission deviates from the square profile, due to the limited bandwidth (~50 kHz) of the APD.

#151983 - $15.00 USD Received 15 Aug 2011; revised 27 Sep 2011; accepted 3 Oct 2011; published 27 Oct 2011

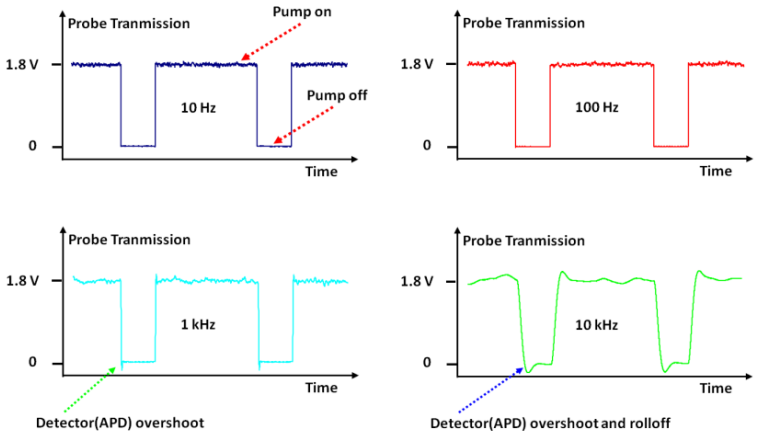

Fig. 6. Low-frequency modulation results for a duty cycle of 70% (on-state), for four different frequencies. At 10 kHz, the signal is limited by the APD bandwidth.

A careful consideration of the physical mechanism behind this modulation reveals that the modulation speed is fundamentally limited by the time needed for the atoms to repopulate the ground state, |a>, after the pump is turned off, so that they can absorb the probe again. This means that the modulation bandwidth cannot exceed the homogeneous linewidth (HL). For the TNF system, the HL is dominated by the transit time broadening, which is about 100 MHz, as shown in Ref. [5[. The HL can be increased very significantly by adding a buffer gas, such as ^{4}He. In a series of studies carried out in the context of the development of diode pumped alkali lasers (DPALs) [27], it has been shown that the atoms excited to the $5P_{3/2}$ state relaxes very rapidly to the $5P_{1/2}$ state. The rate of relaxation from the $5P_{1/2}$ state to the ground state can be augmented by adding an auxiliary, strong beam that would be turned on at the same time as the pump is turned off, and turned off before turning on the pump again. For buffer gas pressure of 1 atm, the HL is about 10 GHz. A HL linewidth as large as 500 GHz is possible in the presence of a buffer gas pressure of 25 atm. Of course, the intensity needed to saturate a 500 GHz broadening would be too hard to realize in a TNF. However, based on a typical DPAL laser in Rb, which requires a threshold pump intensity of about 15 μW/μm^2, a pump power of about 3 μW should be enough the achieve the 10 GHz modulation bandwidth in the TNF, which has a mode area of only 0.2 μm^2. The same level of power would be needed for the auxiliary pump beam for rapid depopulation of $5P_{1/2}$ state to the ground state.

In reference 28, Hendrickson et al. reported a scheme whereby a control beam at 770 nm affects the transmission of a probe beam at 780 nm, when both are passed through a TNF embedded in Rb vapor. This approach is based on non-resonant, thermal effect induced by the pump, and is fundamentally different from the effect we are reporting here. Because of the thermal nature of the effect, it requires a much stronger effect, and is unlikely to work at a high frequency.

6. Future work

The setup shown in Fig. 3 could not be employed for observing high frequency modulations for two reasons. First, the AOM modulation bandwidth is only a few MHz. This could be circumvented by using a high-speed EOM, configured for intensity modulation, and inserting it after the modulator AOM, kept turned on continuously. Second, the bandwidth of the APD used is only about 50 kHz. On the other hand, the high speed detectors we have are not sensitive enough for the 100 pW probe. This limitation can be circumvented by inserting a Fabry-Perot cavity (FPC) in front of the APD. The modulation imparted to the probe would then show up as sidebands of the FPC output as its length is scanned. A constraint of this

#151983 - $15.00 USD Received 15 Aug 2011; revised 27 Sep 2011; accepted 3 Oct 2011; published 27 Oct 2011

approach is that the FPC yields information on the magnitude only of the spectrum of the modulated probe, and not the relative phases between the various spectral components. As such, by itself, this method would not reveal the actual shapes of the probe modulation. An additional EOM and an interferometer would be needed to recover the phase of each spectral component. These modifications, as well as the process of adding a buffer gas to the TNF chamber, are in progress.

7. Conclusion

To summarize, we have demonstrated an ultra-low light level optical modulator using a tapered nano fiber embedded in a hot rubidium vapor. The control and signal beams are co-propagating but orthogonally polarized, leading to a degenerate V-system involving coherent superpositions of Zeeman sublevels. The modulation is due primarily to the quantum Zeno effect for the signal beam induced by the control beam. For a control power of 40 nW and a signal power of 100 pW, we observe near 100% modulation. The ultra-low power level needed for the modulation is due to a combination of the Zeno effect and extreme field localization in the evanescent field around the taper. Efforts are underway to demonstrate modulation speeds of several GHz by adding a buffer gas to the system.

Acknowledgments

This work was supported in part by AFOSR Grant # FA9550-10-01-0228, NSF IGERT Grant # DGE-0801685, and the DARPA ZOE program under Grant # W31P4Q-09-1-0014.

#151983 - $15.00 USD Received 15 Aug 2011; revised 27 Sep 2011; accepted 3 Oct 2011; published 27 Oct 2011